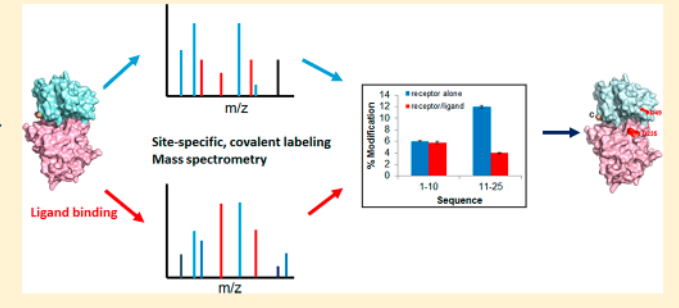
Probing a Plant Plasma Membrane Receptor Kinase's Three-**Dimensional Structure Using Mass Spectrometry-Based Protein** Footprinting

Pei Liu, Miyoshi Haruta, Benjamin B. Minkoff, and Michael R. Sussman*

Department of Biochemistry, Biotechnology Center, University of Wisconsin, Madison, Wisconsin 53706, United States

Supporting Information

ABSTRACT: FERONIA (FER), one of the 17 malectin-like receptor-like kinases encoded in the Arabidopsis genome, acts as a receptor for a 5 kDa growth-inhibiting secreted protein hormone, rapid alkalinization factor 1 (RALF1). Upon binding the peptide ligand, FER is involved in a variety of signaling pathways eliciting ovule fertilization and vegetative root cell expansion. Here, we report the use of mass spectrometry-based, carbodiimide-mediated protein carboxyl group (aspartic and glutamic acid) footprinting to map solvent accessible amino acids of the ectodomain of FER (ectoFER), including those involved in RALF1 binding and/or allosteric



changes. Aspartate and glutamate residues labeled in this procedure were located in various regions, including the N-terminus, malectin-like domains, and juxtamembrane region, and these correlated well with a three-dimensional structural model of ectoFER predicted from the crystal structure of a related receptor. Covalent cross-linking experiments also revealed the Nterminus of ectoFER linked to the highly conserved C-terminus of RALF1. RALF1 binding assays performed with truncation mutants of ectoFER further implicated the receptor N-terminal and juxtamembrane regions in the binding of RALF1. In conclusion, our results of mass spectrometry-based footprinting methods provide a framework for understanding ligand-induced changes in solvent accessibility and their positions within the three-dimensional structure of a plant receptor kinase.

I nlike most animals, plants cannot move to escape adverse environmental conditions. To survive, plant cells have evolved hundreds of sensors and regulators that perceive the extracellular environment and modulate plant developmental programs accordingly. Receptor-like protein kinases (RLKs) are one of the most important regulatory signaling systems in plants, comprising >600 homologous proteins that constitute ~2.5% of the annotated protein-coding genes in the Arabidopsis genome. Despite their abundance, for only a small number of the RLKs is there any molecular understanding of precisely how they interact with ligands, and this list includes a steroid receptor brassinosteroid insensitive 1 (BRI1), flagellin receptor flagellin sensitive 2 (FLS2), a fiveamino acid peptide phytosulfokine (PSK) receptor, PSKR,4 and an endogenous peptide AtPep1 receptor PEPR1.5 RLKs are transmembrane proteins with an extracellular domain, a single transmembrane domain, and a cytoplasmic kinase domain. On the basis of the structural features of their extracellular domains, RLKs can be classified into multiple subfamilies. Catharanthus roseus RLK1-like kinases (CrRLK1L) make up one of the subfamilies that have malectin-like extracellular domains. In Arabidopsis thaliana, there are 17 members, including ANXUR1 (ANX1), ANXUR2 (ANX2), HERCULES1 (HERK1), and HERCULES2 (HERK2). 7,8 These proteins regulate a wide range of biological

processes, including cell wall integrity sensing, regulation of cell expansion, and sexual reproduction.8,5

The FERONIA (FER) receptor kinase, a member of the CrRLK1L subfamily, was named after the fertility goddess, FERONIA, from an Etruscan legend of ancient Italy. The origin of its name arose from the discovery that its ablation causes a fertilization defect. More specifically, in a FER knockout mutant, the pollen tube does not stop elongating growth when it reaches the synergid cells of the ovule, thus causing pollen tube "overgrowth", reduced fertility, and a semisterile phenotype. 10,11 FER is also involved in a variety of other signaling pathways, including vegetative root growth and development, pathogen defense, and hormone-mediated responses.¹² It has been demonstrated that FER acts as a receptor for a small growth-inhibiting secreted peptide known as rapid alkalinization factor 1 (RALF1).13 RALF was first isolated from tobacco leaves as an endogenous growth regulator. It causes rapid alkalinization in the medium of cultured cells and also inhibits seedling root growth. 14,15 Subsequent studies demonstrated that binding of RALF1 to FER initiates a rapid kinase-mediated cascade followed by changes in the phosphorylation status of the regulatory domain

Received: April 23, 2018 Revised: August 6, 2018 Published: August 20, 2018

of the plasma membrane proton pump. This in turn contributes to rapid alkalinization of the apoplast and cessation of cell expansion. 13 On the basis of the amino acid sequence, the ectodomains of FER and other CrRLK are annotated to contain two tandemly repeated malectin-like domains separated by a loop. Malectin is an animal ER-localized protein that recognizes a diglucose moiety. However, the level of amino acid sequence identity between mammalian malectin and the malectin-like region found in the ectodomain of CrRLKs is low (<20%), and it is unclear whether the weak similarity between the animal and plant sequences reflects a bona fide role for sugars in FER-mediated signaling. 16 It is thus important to experimentally characterize the three-dimensional structure and carbohydrate- or peptide-ligand binding sites to be certain whether sugars are involved in CrRLK signaling. The first crystal structures of the ectodomains of the plant CrRLKs, ANXUR1 and ANXUR2, were recently determined without their ligand attached, and this did not provide definitive information about the identity of ligands. 17 Binding of RALFs to the ectodomain of FER and other CrRLKs has been experimentally measured, but the exact amino acid residues involved in binding of the ligand to the peptide hormone have not yet been identified.

To obtain protein three-dimensional structural information, a variety of mass spectrometric-based approaches have been developed, including hydrogen-deuterium exchange (HDX), covalent labeling (CL), and cross-linking (XL). determines solvent accessibility by measuring the rate of hydrogen-to-deuterium exchange within the amide hydrogen on the protein peptide bond backbone. 19,20 Hydroxyl radicalbased labeling is able to target the side chains of a large number of amino acids and offers good coverage of the overall sequence to map protein surfaces.²¹ Another applicable approach for specific, irreversible covalent modification is 1ethyl-3-[3-(dimethylamino)propyl]carbodiimide (EDC)-mediated glycine ethyl ester (GEE) labeling of the carboxyl group of a protein and is specific for identifying aspartate and glutamate residues exposed to solvent. This reaction can lead to quantitative modification of solvent accessible carboxyl groups under aqueous conditions and physiological pH, and it has been widely used to characterize protein surface structure and protein complex analysis. 22,23 Another approach involves chemical cross-linking via bifunctional reagents that link two residues. This creates new intramolecular or intermolecular bonds whose identification then imposes distance constraints on the three-dimensional location of the two amino acid side chains, thereby yielding information about how a single protein or protein complex is folded.24

In vitro studies have demonstrated that the ectodomain of FERONIA (ectoFER) heterologously expressed and purified from Escherichia coli is capable of specifically binding to RALF1.¹³ In the study presented here, we mapped ectoFER's surface solvent accessibility by comparing carboxyl group reactivity before and after RALF1 binding using carbodiimide (EDC)-mediated glycine ethyl ester (GEE) labeling. In addition, to provide assistance in the interpretation of the footprinting experiments, we also utilized chemical cross-linking, RALF1 binding assays, genetic mutations, and computational approaches to predicting FER ectodomain three-dimensional structure based on similarities to known sequences of other malectin receptor ectodomains that were recently crystallized. Overall, our study of ligand-induced changes in FER solvent accessibility by mass spectrometric-

based bottom-up sequence analysis revealed peptide regions and specific amino acids that are likely to be directly involved in binding or in allosterically responding to the bound ligand.

MATERIALS AND METHODS

Protein Purification. Maltose binding protein (MBP) FER ectodomain (MBP-ectoFER) fusion protein was expressed in E. coli and purified with amylose agarose (NEB) according to procedures previously described 13 with a modification that 20 mM sodium phosphate (pH 7.4) instead of 20 mM Tris-HCl was used in the wash and elution steps. His-RALF1 peptide, His-RALF1 ($\Delta 2-8$), and Cys-His-RALF1 were purified from E. coli by Ni-NTA His Bind resin (Novagen) and isolated by a C4 (Vydac) high-performance liquid chromatography (HPLC) step essentially as described previously.²⁵ Truncation mutations were cloned from the aforementioned MBP-ectoFER vector using QuickChange II Site-Directed Mutagenesis Kits (Agilent) or Gibson assembly (NEB) according to the manufacturer's protocol. The primers used in the truncation constructs are listed in Supplementary Table 1. All sequences were verified using Big-Dye Sanger sequencing. The annotated sequences of FER and RALF1 are shown in Supplementary Figure 1.

Carboxyl Group Labeling Reaction and Protein Digestion in Solution. For protein denaturation, 0.5% sodium dodecyl sulfate (SDS) was added to the MBP-ectoFER and incubated at room temperature (RT) for 30 min. RALF1 (5 μ M) and ectoFER (0.5 μ M) were mixed together at different molar ratios and incubated for 30 min at RT before adding carboxyl group labeling reagents. Glycine ethyl ester (GEE) and 1-ethyl-3-[3-(dimethylamino)propyl]carbodiimide hydrochloride (EDC) (Thermo Fisher Scientific, Rockford, IL) were freshly prepared in 20 mM sodium phosphate (pH 7.4) at concentrations of 2 and 0.5 M, respectively. The reaction was initiated by mixing the proteins with GEE and EDC at final concentrations of 35 and 3.5 mM, respectively. The labeling was performed at RT for 1, 2.5, and 5 min or a fixed time point of 2.5 min followed by quenching using an equal volume of sodium acetate (1 M). Three replicates were included for each sample. Labeled samples were precipitated with methanol and chloroform, and the pellet was washed with 80% acetone followed by solubilization in 7 M urea. Dissolved proteins were diluted to 4 M urea with 25 mM ammonium bicarbonate, reduced for 30 min with 5 mM dithiothreitol (DTT) at 42 °C, and alkylated for 45 min with 15 mM iodoacetamide at RT in the dark. Proteins were further diluted to 1.2 M urea with 25 mM ammonium bicarbonate, and equal amounts of trypsin (Promega) and LysC (Wako) were added at a total protein:enzyme ratio of 40:1. The digestion was performed at 37 °C overnight. After digestion, peptides were desalted using OMIX C18 tips (Agilent Technologies) according to the manufacturer's protocol, dried in a vacuum centrifuge, and dissolved in liquid chromatography-mass spectrometry (LC-MS) grade 0.1% formic acid (Fisher

Chemical Cross-Linking and In-Gel Protein Digestion. Three chemical cross-linkers, bis(sulfosuccinimidyl)suberate (BS3), dithiobis(succinimidyl propionate) (DSP), and disuccinimidyl sulfoxide (DSSO), from Thermo Scientific were used in this study. Immediately before application, a BS3 solution was freshly prepared in 20 mM sodium phosphate buffer (pH 7.4), whereas the hydrophobic DSP and DSSO were dissolved in DMSO in accordance with the manufac-

turer's instructions. ectoFER (0.5 μ M) and RALF1 (5 μ M) were incubated with the cross-linker for 30 min at RT, and the reaction was quenched by the addition of 1 M Tris-HCl (pH 7.6) to a final concentration of 100 mM. After quenching, the cross-linked samples and control samples were denatured in NuPAGE LDS Sample Buffer (4x) (Thermo) with 50 mM DTT and incubated at 95 °C for 5 min. Electrophoresis was performed using NuPAGE 4-12% Bis-Tris Protein Gels. Selected bands were excised with a razor blade, cut into 1 mm pieces, and placed in low-protein binding tubes (LoBind, Eppendorf). The gel was reduced with 25 mM DTT at 56 °C for 20 min and alkylated with 55 mM iodoacetamide in the dark for 20 min. Gel pieces were then digested with 200 ng of trypsin (Promega sequence grade modified) in 25 mM ammonium bicarbonate with 0.01% ProteaseMAX Surfactant (Promega). After digestion for 2-3 h at 42 °C, the peptides were recovered and purified with OMIX C18 tips, dried in a vacuum centrifuge, and dissolved in LC-MS grade 0.1% formic acid (Fisher Scientific) for further MS analysis.

Mass Spectrometry. The dissolved peptide was analyzed with a Thermo Orbitrap Elite LC-MS/MS instrument attached to an Agilent 1100 HPLC system. The samples were loaded onto a 150 mm \times 75 μ m Magic C18AQ column with a 200 Å pore size and a 3 μ m particle size (Bruker). The peptides were eluted at a flow rate of 0.5 µL/min from 0 to 30 min of 100% solvent A (0.1% formic acid in water), followed by a rate of 0.3 μ L/min from 31 to 45 min to 60% B (0.1% TFA in acetonitrile), and then from 45 to 50 min to 100% B, maintained at 100% for 5 min, and then re-equilibrated from 56 to 80 min with 100% A. MS1 survey spectra were acquired at a resolving power of 60000 over the m/z range of 350-1800. The top 20 most abundant peptides with +2 or more charge states were selected for MS/MS. Dynamic exclusion was used for 15 s with a repeat count of 2. Precursor ions were fragmented via collision-induced dissociation (CID) with helium using a normalized collision energy of 32 and an isolation window width of m/z 2.0. For DSSO samples, one MS1 scan was followed by two data-dependent MS2 scans in FT mode with CID fragmentation on the top two MS peaks, and three MS3 scans in the LTQ on the top three peaks from each MS2. The normalized collision energy was set at 20 and 35% in MS2 and M3, respectively.

Data Analysis. MS data were processed using Proteome Discoverer (version 2.1) software with the SEQUEST search algorithm and the following parameters: trypsin protease digestion with one missed cleavage allowed, precursor ion tolerance of 15 ppm, and fragment ion tolerance of 0.6 Da. Cysteine carbamidomethylation was set as a fixed modification, and methionine oxidation and asparagine/glutamine deamidation were set as variable modifications. For EDC/GEE labeling samples, the variable modification on glutamate or aspartate was set by adding 85.0528 and 57.0215 Da corresponding to the mass of a GEE-labeled amide and its hydrolyzed product, respectively. Extracted ion chromatograms (EICs) of peptides were derived from MS1 data, and the corresponding peak areas were integrated by Proteome Discoverer. If one peptide contained multiple sites of modification that could not be separated during chromatography or the tandem mass spectrum was not sufficient for assignment of the modification to a single residue, the number of peptide-to-spectrum matches (PSMs) in the MS/MS mode was used to split the chromatogram area. For example, if a peptide had a total of 10 product ion spectra and seven of these were attributed to a

glutamate residue modification, then 70% of the signal area for that peak was attributed to the glutamate modification. The remaining 30% of the signal was attributed to other modifications that produced the three remaining product ion spectra. The raw mass spectrometric data have been deposited at the Chorus project (https://chorusproject.org).

The BS3 cross-linked peptide MS/MS data were analyzed with StavroX (version 3.6) and Proteome Discoverer (version 2.1) with the following general settings: trypsin as the cleavage enzyme with three missed cleavage sites allowed, methionine oxidation and asparagine/glutamine deamidation as variable modifications, and cysteine carbamidomethylation as a static modification. In Proteome Discoverer, RALF1 peptides with a BS3 cross-linker were set as variable modifications for database searches, specifically, GCSK(xl)IAR (+928.4872), GCSK(xl)IARCR (+1244.619), and YISYQSLK(xl)R (+1294.699). For DSP cross-linking, variable modification lysine CAMthiopropanoyl (+145.0198 Da) was also selected. DSSO cross-link data were analyzed with XlinkX.²⁶

Alexa Fluor 488 C5 Maleimide Labeling of CysRALF1 and the Fluorescence Polarization Assay. Alexa Fluor 488 C5 maleimide (Thermo) labeling of CysRALF1 was performed by following the manufacturer's protocol. CysRALF1 (13.5 nmol) was mixed with Alexa Fluor 488 C5 maleimide (130 nmoles) in a 130 μ L solution and incubated at RT for 30 min in the dark. The reaction was terminated by adding 13 μ L of 3% trifluoroacetic acid, and the labeled CysRALF1 was purified by applying the reaction mixture to a PD-10 size exclusion column (GE Healthcare). The column was run with a 0.1% trifluoroacetic acid solution, and 16 fractions (1 mL each) were recovered. The labeling efficiency of Alexa-CysRALF1 was estimated using an absorption spectrometer according to the manufacturer's instructions and matrix-assisted laser desorption ionization time of the flight.

The fluorescence polarization assay was performed in a 384-well black flat bottom plate. Alexa488-CysRALF1 (50 nM) and different concentrations of wild-type ectoFER or 150 nM truncation mutants were mixed in 50 mM sodium phosphate buffer (pH 7.0). Control wells with only 50 nM Alexa488-CysRAFL1 were included for determination of the fluorescence polarization (FP) value of the free peptide. After incubation for 15 min, the FP value of each well was read using a Tecan infinite F500 microplate reader at 485 nm excitation and 535 nm emission with an excitation bandwidth of 20 nm and an emission bandwidth of 25 nm. The *G* factor was set at 1; the number of flashes was 10, and the gain was set to optimal.

RESULTS

EctoFER Surface Structure Analysis. In mass spectrometry-based protein footprinting studies, a high protein sequence coverage is often a critical but challenging goal. Trypsin, the most widely used proteolytic enzyme, could generate only 72% sequence coverage of ectoFER, and the regions lacking spectral identification included two peptides (160–228 and 293–321). Via application of a second protease of different specificity, chymotrypsin, following trypsin digestion, the sequence coverage was increased to 92%. The remaining small amounts of incomplete coverage included small peptides (two to five amino acids) resulting from trypsin and chymotrypsin digestion, which usually elute early in the HPLC separations and escape detection by LC–MS/MS

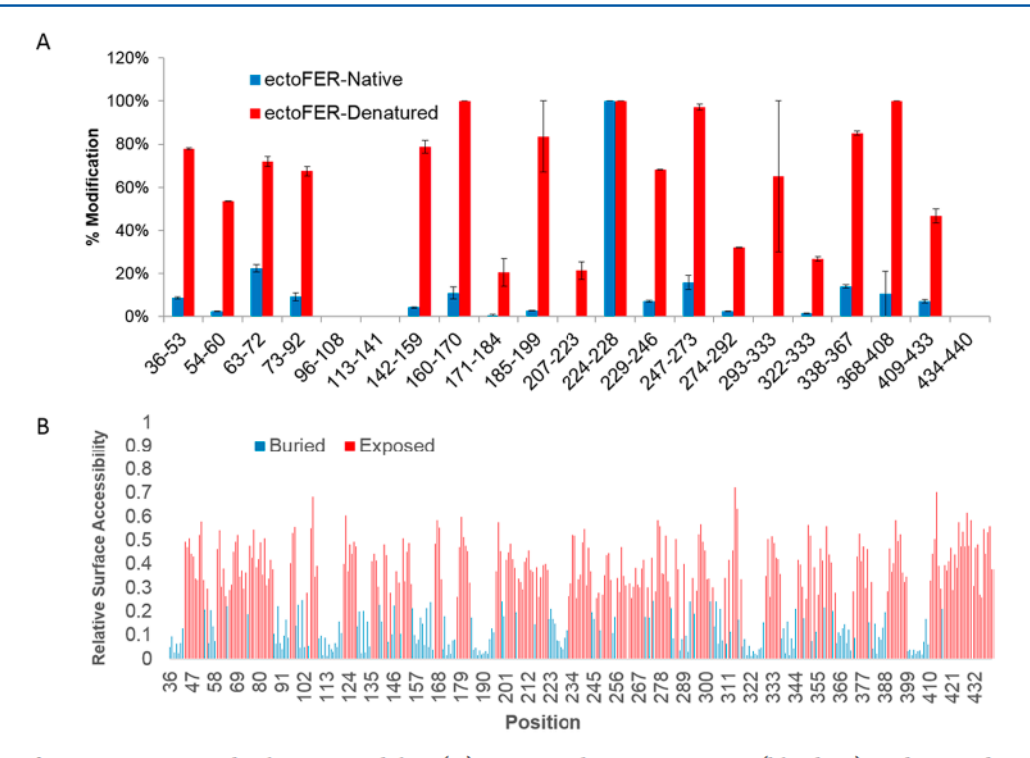


Figure 1. Analysis of ectoFER amino acid solvent accessibility. (A) EctoFER that is in its native (blue bars) or denatured state (red bars) was modified by carbodiimide-based GEE labeling. (B) The ectoFER amino acid surface accessibility was predicted by NetSurfP-1.1. A threshold for the buried amino acid was <0.25 relative surface accessibility. The blue bars represent buried amino acids, and the red bars represent exposed ones. Error bars show the standard deviation, and n = 2.

analysis. The annotated sequences of FER and RALF1 are shown in Supplementary Figure 1.

In this study, 1-ethyl-3-[3-(dimethylamino)propyl]-carbodiimide (EDC)-mediated glycine ethyl ester (GEE) modification of the carboxyl groups of aspartyl (D) and glutamyl (E) residues was used as a footprinting procedure to map the solvent accessibility of amino acid side chains in ectoFER. This method was chosen for the following reasons. (1) There are 23 aspartate and 16 glutamate residues in ectoFER, providing wide coverage of the overall ectoFER sequence to map the protein surface. (2) The reaction can be conducted under physiological conditions. (3) Aspartate and glutamate side chains are often important for protein biochemical functions. (4) The reaction products are stable during sample preparation. (5) The quantitative modification of a carboxyl group is widely accepted as an indication of solvent accessibility.

In the covalent labeling procedures, it is important to check the structural integrity of target proteins during the modification procedure. For this purpose, we performed a preliminary peptide-level time-dependent modification analysis whereby a deviation from linearity of the time course plot would suggest an alteration in protein structure involving the modified residue(s).²⁷ Among the three tested time points (1, 2.5, and 5 min), almost all of the modified peptides had a linear modification response except peptides 63-72 and 338-367 (Supplementary Figure 2). Thus, to maximize structural integrity at all reactive sites, we chose a 2.5 min time point for further experiments. To clearly delineate amino acids involved in protein structure rather than simple chemical reactivity, we compared the EDC/GEE labeling of a fully denatured ectoFER versus the native or folded protein structure. At first, we used predigestion with trypsin as a

type of denaturant. In other words, both samples were digested with trypsin, but the "native" sample was exposed to EDC/ GEE before it was digested while the denatured sample was exposed to EDC/GEE after digestion. Significantly higher extents of modification were found in the predigested ecoFER sample. Because the sequence context may have an effect on amino acid labeling, 28 in separate experiments, sodium dodecyl sulfate (SDS) was also used to denature the protein. The SDSdenatured protein exposed almost all the peptides to the labeling reagents, resulting in a high extent of modification in almost all identified peptides. The peptides from nondenatured ectoFER had a much lower extent of modification, indicating that ectoFER expressed heterologously and purified from E. coli was folded properly (Figure 1A). It should be noted that both native and denatured forms had no significant spectral count differences (Supplementary Figure 3), and thus, the overall pipeline of digestion and mass spectral analysis was not affected by solvent accessibility issues. Although the threedimensional structure of the FER ectodomain (or the rest of the protein) has not yet been determined, to benchmark our experimental studies we attempted to predict the solvent accessibility using NetSurfP-1.1 (http://www.cbs.dtu.dk/ services/NetSurfP/) (Figure 1B). When the amino acid relative surface accessibility is >0.25, the amino acid is regarded as exposed; otherwise, it is buried. On the basis of this threshold, the regions of residues 63-72 and 247-273 that had relatively high extents of modification in the labeling experiments also are predicted to be exposed. E224 in peptide 224-228, which was almost completely labeled in both nondenatured and denatured forms of the protein, is predicted to be buried, located within the extremely flexible loop region between the two malectin domains. Thus, apart from this one peptide, the predicted and observed patterns of solvent

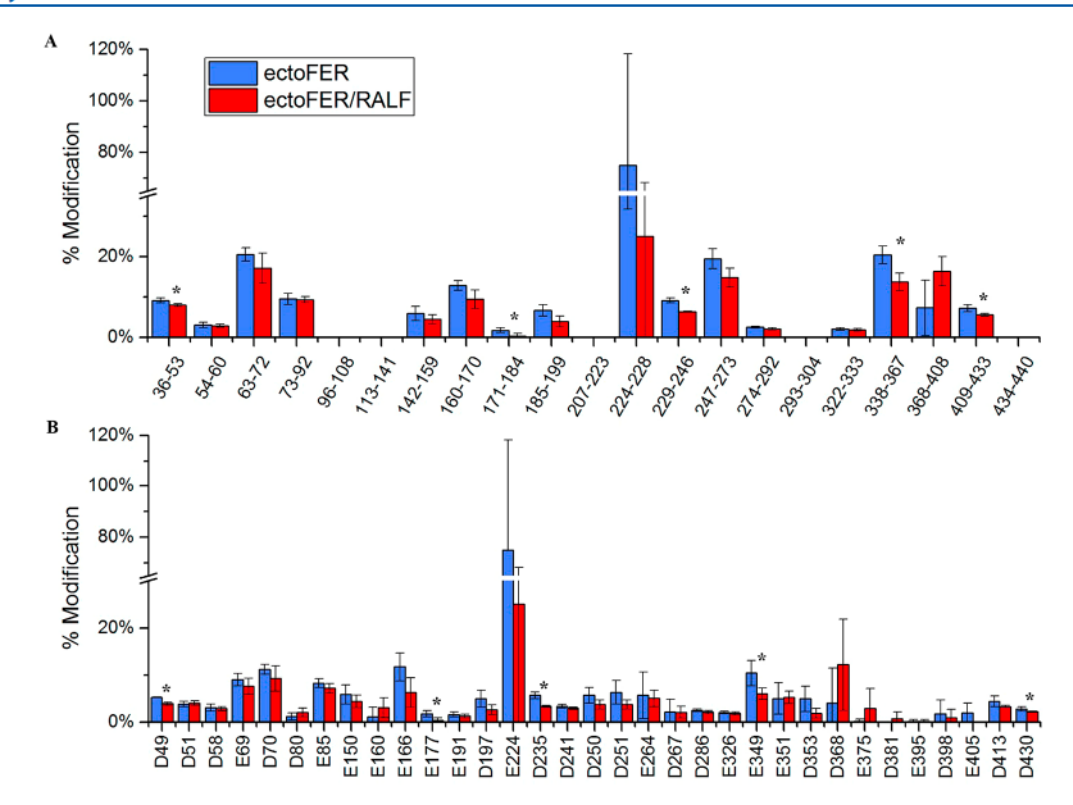


Figure 2. Extents of modification of ectoFER alone (blue bars) or RALF-bound ectoFER (red bars) by GEE/EDC labeling. (A) Extent of modification at the peptide level. (B) Extent of modification at the residue level. The blue bars show data for ectoFER alone, and the red bars show data for ectoFER with RALF1. Asterisks indicate residues with statistically significant changes (p < 0.05; t test). Error bars show the standard deviation, and n = 4.

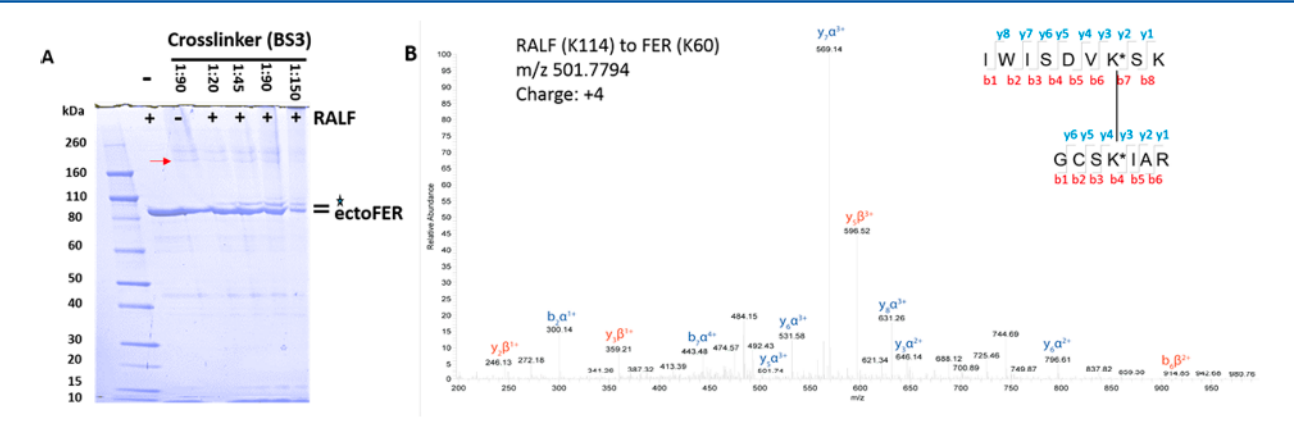


Figure 3. BS3 cross-linking analysis of ectoFER and RALF1. (A) SDS-PAGE analysis of ectoFER and RALF1 with the indicated protein:BS3 molar ratio. EctoFER was the only band observed before the addition of cross-linker BS3. After cross-linking, a new, high-molecular weight band appeared, corresponding to the cross-linked ectoFER and RALF1 (asterisk). A much higher-molecular weight band that may be the dimer of ectoFER also was observed in the presence of a cross-linker with or without RALF1 binding (red arrow). (B) Tandem mass spectrum of K114 of RALF1 linked to K60 of ectoFER.

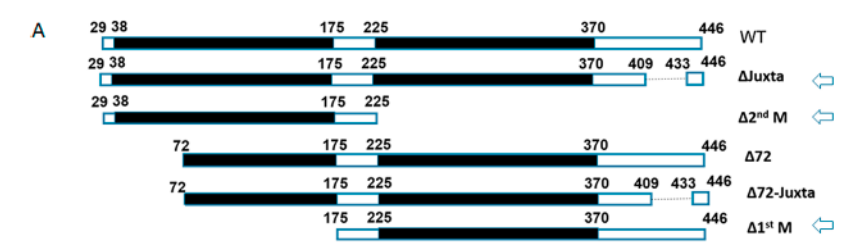
accessibility across the protein are self- consistent, suggesting that the predicted structure, as a first approximation at least, is reflective of a plausible three-dimensional structure.

Labeling of the EctoFER and RALF1 Complex with EDC/GEE at the Peptide and Amino Acid Levels. To study potential conformational changes in ectoFER induced by RALF1 binding, carboxyl group labeling of ectoFER before and after RALF1 binding was compared. Because there are no glutamyl or aspartyl residues in the RALF1 sequence, we focused on ectoFER modifications. When ectoFER bound with RALF1 was compared to ectoFER alone, there was a significant decrease in the extent of modification of peptides

at amino acid positions 36–53, 171–199, 229–246, 338–367, and 409–433, with two in the first malectin-like domain, two in the second malectin-like domain, and one in the juxtamembrane region (Figure 2A). Other modified peptides showed no significant differences before and after RALF1 binding.

In this study, 18 aspartate and 15 glutamate residues were modified of a total of 23 aspartate and 16 glutamate residues in the ectodomain of FER. The residues that were not modified included those few that lacked identification in our mass spectrometry pipeline. Some residues that could not be labeled with or without RALF1 binding may be constitutively buried,

Biochemistry



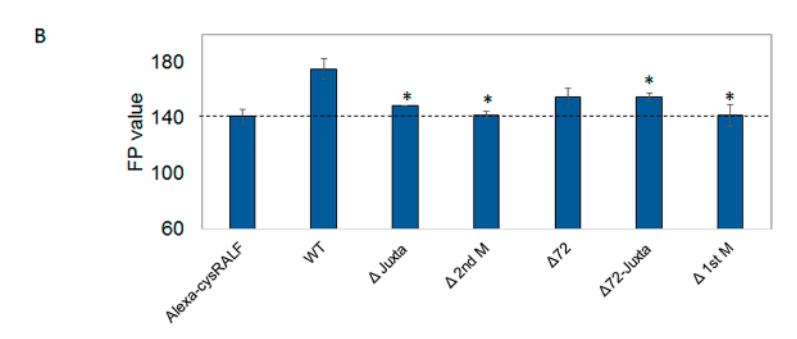


Figure 4. Fluorescence polarization assay of Alexa-CysRALF1 with wild-type ectoFER and its truncation mutants. (A) Schematic diagrams of different truncation mutants of ectoFER. The two black regions spanning amino acid residues 38-175 and 225-370 are malectin-like domains. (B) Fluorescence polarization values of Alexa-CysRALF1 after the addition of different truncation ectoFER mutations. Asterisks indicate residues with statistically significant changes (p < 0.05; t = 0.05). Error bars show the standard deviation, and t = 0.05.

e.g., D121 in a peptide containing amino acids 113–141. Although charged amino acids are usually located on the surface of protein, some microenvironments may completely block the solvent accessibility of these residues. We found that residues D49, E177, D235, E349, and D430 were significantly decreased in their level of labeling with EDC/GEE after RALF1 binding (Figure 2B). These sites may thus be directly involved in the binding interface of RALF1 and FER or allosterically involved in the conformational changes within FER that occur after RALF1 binding.

Mapping EctoFER and RALF1 Binding by Covalent Cross-Linking and Mass Spectrometry. Because RALF1 lacks glutamate or aspartate, the EDC/GEE covalent labeling method was unable to provide information about which region of RALF1 binds to ectoFER. To investigate this question, we applied MS/MS methods after chemical cross-linking. Three chemical cross-linkers were tested, bis(sulfosuccinimidyl)suberate (BS3), dithiobis(succinimidyl propionate) (DSP), and disuccinimidyl sulfoxide (DSSO), which are all homobifunctional protein cross-linkers with targeted reactivity toward primary amines. Cross-linked ectoFER and RALF1 molecules were separated by sodium dodecyl sulfatepolyacrylamide gel electrophoresis (SDS-PAGE) and visualized by Coomassie Blue staining. The individual MBPectoFER (~90 kDa) and RALF1 (~6 kDa) species could be seen as separate bands before the addition of cross-linkers, but after cross-linking, the intensity of these individual bands decreased and a new, high-molecular weight band between 90 and 110 kDa appeared. This new band appeared with increasing concentrations of cross-linker at the molecular weight predicted for an RALF1-ectoFER complex (Figure 3A). At the same time, a higher-molecular weight band appeared around 200 kDa, which may correspond to an ectoFER dimer.

A major concern about protein cross-linking is whether the use of an excess of cross-linkers will affect the conformation of the proteins. To address this potential problem, we tested different cross-linker:protein concentration ratios. With an

increased BS3:ectoFER ratio, there was an increased intensity of cross-linked bands and a maximum peak at a 90:1 crosslinker:protein ratio (Figure 3A). To test whether the observed cross-linked band was specifically caused by covalent linkage of ectoFER and RALF1, the biologically inactive ($\Delta 2$ –8) RALF1 was used as a negative control. We compared different protein:ligand concentration ratios (1:2, 1:5, and 1:10) as indicated in Supplementary Figure 5. The results showed that although ($\Delta 2$ -8) RALF1 also caused the same cross-linked band, it occurred with a 50% lower efficiency. After ectoFER and RALF1 were cross-linked by DSP, the proteins were loaded on a SDS-PAGE gel with (reducing) or without DTT (nonreducing). As expected, because DSP has a cleavable disulfide bond in its spacer arm, we observed that the DSP cross-linked band disappeared after the addition of DTT, and the ectoFER band intensity recovered (Supplementary Figure 6B). Furthermore, when the cross-linked band was analyzed by mass spectrometry, only ectoFER and RALF1 sequences were identified. In summary, these results suggest that the crosslinked band (90K-110K) is caused by a biologically meaningful interaction between ectoFER and RALF1.

To identify ectoFER and RALF1 peptide sequences localized at the binding surface, the cross-linked ectoFER-RALF1 band was cut from the gel and digested with trypsin, followed by LC-MS/MS sequencing. As a control, ectoFER alone, i.e., with the cross-linker but without RALF1 binding, was also included. The BS3 cross-linked data were analyzed with StavroX (version 3.6.6) and Proteome Discoverer (version 2.1), and DSSO data were searched by XlinkX. The results showed that K60 in 54-IWISDVK(xl)SK-62 of ectoFER was cross-linked to RALF1 K114 in 111-GCSK(xl)IAR-117. Figure 3B shows a representative tandem mass spectrum of the cross-linked peptides with a precursor ion at m/z 501.779 (charge of +4). When 111-GCSK(xl)IAR-117 was set as a modification for normal database searches in Proteome Discoverer, the same result was observed. Similar results were obtained using DSP as a cross-linker. The product ion

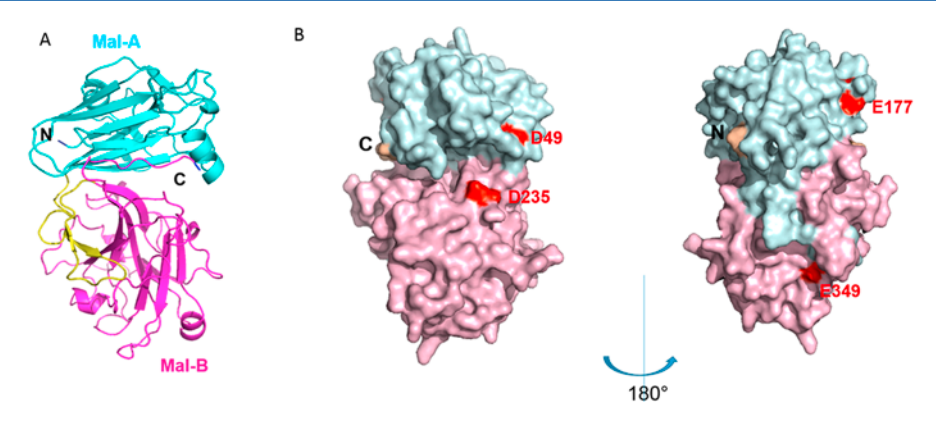


Figure 5. EctoFER structure prediction based on the known structure of ANXUR1. (A) Cartoon diagram of ectoFER based on homology modeling with 5Y96 (ANXUR1) as the template. Malectin-like domain A is colored cyan, malectin-like domain B magenta, and the β -hairpin yellow. (B) EctoFER molecule shown as a surface model. The N- and C-termini are labeled with N and C, respectively. The residues significantly changed by EDC/GEE labeling upon RALF1 binding are colored red.

(MS/MS) spectra are shown in panels C and D of Supplementary Figure 6.

After CID cleavage, the DSSO cross-linked peptide $\alpha-\beta$ could be separated into a pair of peptide fragments (α_A/β_S) or α_S/β_A , in which the α peptide fragment is linked with the alkene (A) moiety (+54 Da) and the β peptide fragment is linked with the sulfenic acid (S) moiety (+104 Da) or vice versa. In addition, the sulfenic acid-containing fragment (α_S, β_S) may lose a water molecule (-18 Da) to generate a new fragment containing an unsaturated thiol (T) moiety (+86 Da) (α_T, β_T) . Because of this, there is a mass difference (Δ 32 Da) between the T- and A-modified forms of the same sequence. Supplementary Figure 7 shows a representative pattern of four peaks in MS2 $(\alpha_A/\alpha_T \beta_S/\beta_T)$ after DSSO cleavage by CID fragmentation $[\alpha, IWISDVK(xl)SK; \beta, GCSK(xl)IAR]$. The +4 charged parent ion $(m/z 506.76^{4+})$ generated two pairs of doubly charged ions, α_A^{2+} (565.31²⁺) and α_T^{2+} (581.30²⁺), and β_S^{2+} (423.22²⁺) and β_T^{2+} (439.20²⁺).

Mutation Binding Assay. On the basis of the EDC/GEE footprinting and cross-linking results, it was predicted that the N-terminus, the extracellular juxtamembrane domain, and two malectin-like domains of ectoFER all may play important roles in RALF1 binding. To test this, ectoFER mutants containing different sequence truncations were constructed, expressed, and purified from $E.\ coli$ (Figure 4A): (1) Δ Juxta, from which the juxtamembrane domain (409–433) has been deleted; (2) Δ second M, from which the second malectin-like domain has been deleted; (3) Δ 72, from which the first malectin-like domain (36–72) has been deleted; (4) Δ 72-Juxta, from which the first malectin-like domain (36–72) and juxtamembrane domain (409–433) have been deleted; (5) Δ first M, from which the first malectin-like domain has been deleted.

Fluorescence polarization assays are based on the measurement of molecular rotation in solution and have been used to study the molecular interactions of proteins. To apply this method to measure the binding of RALF1 to the wild-type and mutant ectoFER proteins, we inserted a Cys residue at the amino terminus of RALF1 protein and labeled it with Alexa Fluor 488 (AF488) via Cys maleimide chemistry. The retention of biological activity of CysRALF1 after fluorescent labeling was confirmed by an aequorin calcium assay in intact seedlings (Supplementary Figure 8). For the *in vitro* binding assay, upon excitation with polarized light, the emitted light was depolarized and gave rise to a low FP value in the Alexa-

labeled CysRALF1 measurement under a control condition without addition of the receptor. After the Alexa-labeled CysRALF1 was bound to ectoFER, the movement of the Alexa-labeled CysRALF1 became slower because of an increased molecular mass. Thus, emission signals from the Alexa CysRALF1 bound by ectoFER remain polarized and caused an increased FP value. First, we compared the fluorescence polarization assay of Alexa-CysRALF1 with different concentrations of wild-type ectoFER (Supplementary Figure 9). When the protein: ligand ratio was 3:1, $\leq 80\%$ of the ligand was bound. For this reason, we chose a 3:1 protein: ligand ratio for further mutant experiments. The results showed that Δ first M and Δ second M mutants have the same FP value as the Alexa-CysRALF1 only sample, which indicates that the ectodomain of FER lacking either malectinlike domain would reduce the level of RALF1 binding. On the basis of a statistical analysis, there was no significant FP difference between the $\Delta 72$ mutant and WT, but the $\Delta 72$ -Juxta mutant that lacks the N- and C-termini of the ectoFER had a significantly lower FP signal, suggesting that the Nterminus and juxtamembrane domain both play an important role in RALF1 binding (Figure 4B). Although the Δ 72 and Δ 72-Juxta mutants had similar FP values, there was a lack of statistical significance with the $\Delta 72$ mutant, caused by a large FP measurement variance. Thus, although we cannot say this with certainty, it is possible that the lack of the N-termini of ectoFER alone also impacts RALF1 binding. The detailed FP assay results are listed in Supplementary Table 1. These binding assay results with truncation mutants are consistent with the EDC/GEE labeling and cross-linking results and suggest that the malectin-like domains are important for the structural integrity of ectoFER and that the N-terminus and Cterminus (juxtamembrane domain) are essential for RALF1

EctoFER Structure Determined via Computational Modeling. Recently, the three-dimensional structures of the ectodomains of two CrRLK1L members, ANXUR1 and ANXUR2, were determined by X-ray crystallography. On the basis of the ANXUR1 ectodomain structure, we generated a three-dimensional structure for ectoFER by homology modeling using SWISS Model (Figure 5A). The model shows a structure similar to that of the two ANXURs with two malectin-like domains consisting of four antiparallel β-sheets of each, connected by loops and a β-hairpin linker, and

Biochemistry

the C-terminal tail of ectodomain folds back and interacts with malectin-like domain A. A deep cleft located at the interface between the two malectin-like domains is also found in the structural model of ectoFER. When the carboxyl-containing residues that showed significant changes in EDC/GEE labeling after RALF1 addition were mapped to the model, D49 and D235 are located at the same side as the N-terminus and right at the entrance to the cleft that could be directly involved in binding ligands. E177 and E349 are located at the opposite sides of the cleft. The decreased level of labeling of these two sites could be caused by the conformational change in ectoFER upon RALF1 binding. Because the predicted structure sequence was limited up to amino acid 410, D430 was not mapped (Figure 5B).

DISCUSSION

FERONIA (FER), one of the membrane receptor-like kinases with a malectin-like ectodomain, a single transmembrane domain, and a cytoplasmic kinase domain, has been reported to mediate the rapid protein phosphorylation cascade that occurs after RALF1 is added to plant cells. RALF1-FER binding triggers a downstream signaling cascade that leads to a rapid cytoplasmic calcium increase, apoplastic pH alkalinization, and inhibition of cell elongation. 13 While the genetic function of FER has been studied well in situ, little information about the three-dimensional structure of this important protein and how this structure is involved with ligand occupancy and subsequent protein conformational changes leading to the biological effects is available. Mass spectrometry-based protein footprinting has emerged as a powerful structural biology tool because of its sensitivity, mass accuracy, and fast data analysis.²⁹ EDC-mediated GEE carboxyl group labeling has been widely used to determine the solvent accessibility at various carboxylic acid sites. 23,27 EDC is well-known as a zerolength carbodiimide cross-linker that can activate carboxyl groups to react with primary amines. However, in the presence of a large amount of GEE, the EDC-triggered GEE modification reactions essentially eliminate formation of lysine (K)-D/E cross-links. The reactivity of EDC-mediated GEE modification is thus proportionally related to the D/E solvent

In vitro binding studies have shown that the FER ectodomain produced from E. coli could specifically bind to RALF1.13 The same purified ectoFER sequence was used for the in vitro protein surface solvent accessibility study reported herein. After RALF1 binding, five carboxyl-containing amino acids, i.e., D49, E177, D235, E349, and D430 in ectoFER, exhibited significantly decreased levels of EDC/GEE labeling. Chemical cross-linking results further demonstrated that a FER peptide containing K60 was linked to RALF1, which is adjacent to the D49 that was found to be protected from EDC/GEE labeling after RALF1 binding. It has been reported that a mutation of a glycine residue to aspartic acid (G37D) at the N-terminus of THESEUS, another member of the CrRLK1L superfamily, resulted in a loss of function mutation of this protein.³⁰ The glycine residue is conserved in the CrRLK1L family and corresponds to G41 in FER, which is in peptide 36-53 identified by EDC/GEE labeling near the cross-linked sites. In our three-dimensional structural prediction, D49 is also located at the entrance of the predicted ectoFER cleft, which may suggest that D49 is right at the binding interface between RALF1 and ectoFER. Moreover, a truncation mutation analysis further revealed that deletions of the N-terminus and C-termini caused a significant decrease in RALF1 binding efficiency. Juxtamembrane domains often play a role in receptor kinase signaling. For example, deletion of the juxtamembrane domain in membrane-anchored heparin binding EGF-like growth factor causes a loss of ligand diphtheria toxin binding activity. It is thus possible that the juxtamembrane domain (C-terminus) in ectoFER likewise plays an essential role in ligand binding. The predicted ectoFER structure model based on ANXUR1 and ANXUR2 further revealed that both malectin-like domains are involved in cleft formation. This model is also consistent with our observation that deletion of either malectin-like domain caused a reduction in the level of binding of ectoFER to RALF1.

Chemical cross-linking results further showed that K114 in peptide "111-GCSK(xl)IAR-117" of RALF1 at the highly conserved C-terminus may be be close to the ectoFer binding site. There are more than 30 RALF-like genes in the Arabidopsis genome. 15 It is still unclear whether all RALF peptides interact with FER or FER-related receptor kinases. Recently, RALF1 and RALF23 were shown to interact with and RALF4 and RALF19 were demonstrated to be the ligands of ANXUR1 and ANXUR2.33 It will thus be interesting to investigate how different RALFs interact with the binding sites of various members of the CrRLK1L family to mediate different downstream signaling pathways. Furthermore, some plant pathogenic fungi also contain a functional homologue of plant RALF peptides that is used to "hijack" the plant's own RALF signaling pathway.³⁴ The exogenous RALF peptides secreted by plant pathogens show a conserved Cterminus, implying that the C-terminus of RALF family peptides may be critical for functional specificity.

The presence of malectin-like domains in ectoFER has led to speculation that the ligands could be carbohydrates or glycopeptides. The mature RALF1 peptide lacks predicted N- or O-linked glycosylation sites, and RALF1 peptides both isolated from plants and produced in E. coli also lack glycosylation and are still able to bind to FER. The ectodomain of FER itself is also modified by glycosylation in vivo but not in E. coli where it is heterologously expressed and purified for the studies reported herein. Because it binds to RALF1, glycosylation of FER itself does not appear to be essential for the in vitro assays, although we cannot be certain that their affinity in vitro is as high as that observed with the in vivo glycosylated forms. RALF1 itself is also not expressed in pollen where FER has a function during pollen tube reception.³⁵ Other members of the RALF peptide family may serve as ligands in pollen. Alternatively, it is also possible that FER may have more than one ligand, as frequently observed in mammalian receptor proteins.³⁶ It has also been reported that the extracellular domain of FER can interact directly with pectin in vitro, which provides a model by which FER senses cell wall integrity, although the specificity of this interaction or its relevance to the biological function of FER remains unknown.37 Further in vivo or in vitro covalent labeling experiments are needed to more conclusively determine whether carbohydrates or peptide ligands with glycosylation sites have the same recognition mechanisms as RALF1 produced in E. coli.

Computational analysis revealed that the transmembrane domain of FER contains two GxxxG-like motifs that often drive helix—helix association,³⁸ suggesting that this protein may dimerize under certain conditions. Our cross-link results also showed a higher-molecular weight band between 160 and

260 kDa in the SDS-PAGE gel after the addition of a crosslinker in both ectoFER alone and ectoFER with RALF1 binding samples, which may correspond to the dimer of ectoFER. Ligand-induced dimerization and co-receptor requirements are important mechanisms for activating RLK signal perception and transmission, promoting signal transduction through conformational changes and leading to kinase domain activation via auto- or transphosphorylation.³⁹ The highly studied human epidermal growth factor receptor (EGFR) has an ability to form a dimer and exists as a preformed dimer on the cell surface. The plant receptor kinase, FLS2, has also been shown to form a homodimer regardless of flg22 binding.⁴² Like other RLKs, FER may form oligomers for activation. It is also worth noting that there indeed are a few putative co-receptors for FER, such as LLG1, a glycosylphosphatidyl inositol-anchored membrane protein, which acts as a "chaperone" that helps to deliver FER to the plasma membrane and binds to the extracellular juxtamembrane region of FER.⁴³ It has also been reported that RPM1induced protein kinase (RIPK), a receptor-like cytoplasmic kinase, directly interacts with FER in response to RALF1.44 Given the likelihood that necessary chaperones, co-receptors, or glycosylation modifications are absent in E. coli, the source of all proteins utilized in this study, further in planta experiments are needed to validate the predictions of this in vitro work and to more comprehensively characterize the signal transduction mechanism initiated in plasma membrane receptors in the intact organism.

ASSOCIATED CONTENT

Supporting Information

The Supporting Information is available free of charge on the ACS Publications website at DOI: 10.1021/acs.bio-chem.8b00471.

Sequence diagram of RALF1 and FERONIA, time course modification of ectoFER GEE/EDC labeling, number of peptide to spectrum matches (PSMs) of native or denatured ectoFER, PSMs of carbodiimide-based GEE labeling of ectoFER with or without RALF1, BS3 cross-linking analysis of ectoFER and RALF1 or ΔRALF1, MS-coupled cross-linking analysis of ectoFER with RALF1 by DSP, DSSO cross-linking analysis of ectoFER and RALF1, cytoplasmic calcium assay of Alexa 488-labeled RALF1, FP assay of Alexa-CysRALF1 with wild-type ectoFER, FP assay results of Alexa-CysRALF1 with wild-type ectoFER and its truncation mutants, and primers used in the study for mutation constructs (PDF)

AUTHOR INFORMATION

Corresponding Author

*University of Wisconsin, 425 Henry Mall, Madison, WI 53706. Phone: 608-262-8608. E-mail: msussman@wisc.edu.

ORCID

Pei Liu: 0000-0001-7538-9098

Funding

This work was funded by a grant to M.R.S. from the National Science Foundation (MCB 1713899).

Notes

The authors declare no competing financial interest.

ACKNOWLEDGMENTS

The authors acknowledge the University of Wisconsin—Madison Biotechnology Center Mass Spectrometry Facility for the mass spectrometry analysis, especially Greg Sabat for help with data collection and analysis. The authors also thank Peter Belshaw for advice on peptide modification and the fluorescence-based protein interaction assay, Heather Burch for help with CysRALF1 purification, and Thao Nguyen for protein cross-linking assistance.

ABBREVIATIONS

RLKs, receptor-like kinases; CrRLK1L, *C. roseus* RLK1-like kinase; FER, FERONIA; ectoFER, ectodomain of FERONIA; RALF1, rapid alkalinization factor 1; EDC, carbodiimide; GEE, glycine ethyl ester.

REFERENCES

- (1) Shiu, S. H., and Bleecker, A. B. (2001) Receptor-like kinases from Arabidopsis form a monophyletic gene family related to animal receptor kinases. *Proc. Natl. Acad. Sci. U. S. A.* 98, 10763–10768.
- (2) Wang, Z. Y., Seto, H., Fujioka, S., Yoshida, S., and Chory, J. (2001) BRI1 is a critical component of a plasma-membrane receptor for plant steroids. *Nature* 410, 380–383.
- (3) Chinchilla, D., Bauer, Z., Regenass, M., Boller, T., and Felix, G. (2006) The Arabidopsis receptor kinase FLS2 binds flg22 and determines the specificity of flagellin perception. *Plant Cell* 18, 465–476.
- (4) Matsubayashi, Y., Ogawa, M., Morita, A., and Sakagami, Y. (2002) An LRR receptor kinase involved in perception of a peptide plant hormone, phytosulfokine. *Science* 296, 1470–1472.
- (5) Tang, J., Han, Z., Sun, Y., Zhang, H., Gong, X., and Chai, J. (2015) Structural basis for recognition of an endogenous peptide by the plant receptor kinase PEPR1. *Cell Res.* 25, 110–120.
- (6) Walker, J. C. (1994) Structure and function of the receptor-like protein kinases of higher plants. *Plant Mol. Biol.* 26, 1599–1609.
- (7) Nissen, K. S., Willats, W. G. T., and Malinovsky, F. G. (2016) Understanding CrRLK1L Function: Cell Walls and Growth Control. *Trends Plant Sci.* 21, 516–527.
- (8) Boisson-Dernier, A., Kessler, S. A., and Grossniklaus, U. (2011) The walls have ears: the role of plant CrRLK1Ls in sensing and transducing extracellular signals. *J. Exp. Bot.* 62, 1581–1591.
- (9) Lindner, H., Muller, L. M., Boisson-Dernier, A., and Grossniklaus, U. (2012) CrRLK1L receptor-like kinases: not just another brick in the wall. *Curr. Opin. Plant Biol.* 15, 659–669.
- (10) Escobar-Restrepo, J. M., Huck, N., Kessler, S., Gagliardini, V., Gheyselinck, J., Yang, W. C., and Grossniklaus, U. (2007) The FERONIA receptor-like kinase mediates male-female interactions during pollen tube reception. *Science* 317, 656–660.
- (11) Huck, N., Moore, J. M., Federer, M., and Grossniklaus, U. (2003) The Arabidopsis mutant feronia disrupts the female gametophytic control of pollen tube reception. *Development 130*, 2149–2159.
- (12) Li, C., Wu, H.-M., and Cheung, A. Y. (2016) FERONIA and Her Pals: Functions and Mechanisms. *Plant Physiol.* 171, 2379–2392.
- (13) Haruta, M., Sabat, G., Stecker, K., Minkoff, B. B., and Sussman, M. R. (2014) A peptide hormone and its receptor protein kinase regulate plant cell expansion. *Science* 343, 408–411.
- (14) Pearce, G., Moura, D. S., Stratmann, J., and Ryan, C. A., Jr. (2001) RALF, a 5-kDa ubiquitous polypeptide in plants, arrests root growth and development. *Proc. Natl. Acad. Sci. U. S. A.* 98, 12843–12847.
- (15) Murphy, E., and De Smet, I. (2014) Understanding the RALF family: a tale of many species. *Trends Plant Sci.* 19, 664-671.
- (16) Schallus, T., Jaeckh, C., Feher, K., Palma, A. S., Liu, Y., Simpson, J. C., Mackeen, M., Stier, G., Gibson, T. J., Feizi, T., Pieler, T., and Muhle-Goll, C. (2008) Malectin: a novel carbohydrate-binding protein of the endoplasmic reticulum and a candidate player

in the early steps of protein N-glycosylation. Mol. Biol. Cell 19, 3404—3414.

- (17) Du, S., Qu, L. J., and Xiao, J. (2018) Crystal structures of the extracellular domains of the CrRLK1L receptor-like kinases ANXUR1 and ANXUR2. *Protein Sci.* 27, 886–892.
- (18) Rajabi, K., Ashcroft, A. E., and Radford, S. E. (2015) Mass spectrometric methods to analyze the structural organization of macromolecular complexes. *Methods* 89, 13–21.
- (19) Marcsisin, S. R., and Engen, J. R. (2010) Hydrogen exchange mass spectrometry: what is it and what can it tell us? *Anal. Bioanal. Chem.* 397, 967–972.
- (20) Houde, D., Berkowitz, S. A., and Engen, J. R. (2011) The utility of hydrogen/deuterium exchange mass spectrometry in biopharmaceutical comparability studies. *J. Pharm. Sci.* 100, 2071–2086.
- (21) Xu, G., and Chance, M. R. (2007) Hydroxyl radical-mediated modification of proteins as probes for structural proteomics. *Chem. Rev.* 107, 3514–3543.
- (22) Wen, J., Zhang, H., Gross, M. L., and Blankenship, R. E. (2009) Membrane orientation of the FMO antenna protein from Chlorobaculum tepidum as determined by mass spectrometry-based footprinting. *Proc. Natl. Acad. Sci. U. S. A. 106*, 6134–6139.
- (23) Zhang, H., Shen, W., Rempel, D., Monsey, J., Vidavsky, I., Gross, M. L., and Bose, R. (2011) Carboxyl-group footprinting maps the dimerization interface and phosphorylation-induced conformational changes of a membrane-associated tyrosine kinase. *Mol. Cell. Proteomics* 10, 21.
- (24) Sinz, A. (2006) Chemical cross-linking and mass spectrometry to map three-dimensional protein structures and protein-protein interactions. *Mass Spectrom. Rev.* 25, 663–682.
- (25) Haruta, M., Monshausen, G., Gilroy, S., and Sussman, M. R. (2008) A cytoplasmic Ca2+ functional assay for identifying and purifying endogenous cell signaling peptides in Arabidopsis seedlings: identification of AtRALF1 peptide. *Biochemistry* 47, 6311–6321.
- (26) Liu, F., Rijkers, D. T., Post, H., and Heck, A. J. (2015) Proteome-wide profiling of protein assemblies by cross-linking mass spectrometry. *Nat. Methods* 12, 1179–1184.
- (27) Kaur, P., Tomechko, S. E., Kiselar, J., Shi, W., Deperalta, G., Wecksler, A. T., Gokulrangan, G., Ling, V., and Chance, M. R. (2015) Characterizing monoclonal antibody structure by carboxyl group footprinting. *MAbs* 7, 540–552.
- (28) Xie, B., Sood, A., Woods, R. J., and Sharp, J. S. (2017) Quantitative Protein Topography Measurements by High Resolution Hydroxyl Radical Protein Footprinting Enable Accurate Molecular Model Selection. *Sci. Rep.* 7, 017–04689.
- (29) Wang, L., and Chance, M. R. (2011) Structural mass spectrometry of proteins using hydroxyl radical based protein footprinting. *Anal. Chem.* 83, 7234–7241.
- (30) Hematy, K., Sado, P. E., Van Tuinen, A., Rochange, S., Desnos, T., Balzergue, S., Pelletier, S., Renou, J. P., and Hofte, H. (2007) A receptor-like kinase mediates the response of Arabidopsis cells to the inhibition of cellulose synthesis. *Curr. Biol.* 17, 922–931.
- (31) Nakamura, K., Mitamura, T., Takahashi, T., Kobayashi, T., and Mekada, E. (2000) Importance of the major extracellular domain of CD9 and the epidermal growth factor (EGF)-like domain of heparinbinding EGF-like growth factor for up-regulation of binding and activity. J. Biol. Chem. 275, 18284—18290.
- (32) Stegmann, M., Monaghan, J., Smakowska-Luzan, E., Rovenich, H., Lehner, A., Holton, N., Belkhadir, Y., and Zipfel, C. (2017) The receptor kinase FER is a RALF-regulated scaffold controlling plant immune signaling. *Science* 355, 287–289.
- (33) Ge, Z., Bergonci, T., Zhao, Y., Zou, Y., Du, S., Liu, M. C., Luo, X., Ruan, H., Garcia-Valencia, L. E., Zhong, S., Hou, S., Huang, Q., Lai, L., Moura, D. S., Gu, H., Dong, J., Wu, H. M., Dresselhaus, T., Xiao, J., Cheung, A. Y., and Qu, L. J. (2017) Arabidopsis pollen tube integrity and sperm release are regulated by RALF-mediated signaling. *Science* 358, 1596–1600.
- (34) Thynne, E., Saur, I. M. L., Simbaqueba, J., Ogilvie, H. A., Gonzalez-Cendales, Y., Mead, O., Taranto, A., Catanzariti, A. M., McDonald, M. C., Schwessinger, B., Jones, D. A., Rathjen, J. P., and

Solomon, P. S. (2017) Fungal phytopathogens encode functional homologues of plant rapid alkalinization factor (RALF) peptides. *Mol. Plant Pathol.* 18, 811–824.

- (35) Kessler, S. A., Lindner, H., Jones, D. S., and Grossniklaus, U. (2015) Functional analysis of related CrRLK1L receptor-like kinases in pollen tube reception. *EMBO Rep.* 16, 107–115.
- (36) Kahsai, A. W., Xiao, K., Rajagopal, S., Ahn, S., Shukla, A. K., Sun, J., Oas, T. G., and Lefkowitz, R. J. (2011) Multiple ligand-specific conformations of the beta2-adrenergic receptor. *Nat. Chem. Biol.* 7, 692–700.
- (37) Feng, W., Kita, D., Peaucelle, A., Cartwright, H. N., Doan, V., Duan, Q., Liu, M. C., Maman, J., Steinhorst, L., Schmitz-Thom, I., Yvon, R., Kudla, J., Wu, H. M., Cheung, A. Y., and Dinneny, J. R. (2018) The FERONIA Receptor Kinase Maintains Cell-Wall Integrity during Salt Stress through Ca(2+) Signaling. *Curr. Biol.* 28, 666.
- (38) Mueller, B. K., Subramaniam, S., and Senes, A. (2014) A frequent, GxxxG-mediated, transmembrane association motif is optimized for the formation of interhelical Calpha-H hydrogen bonds. *Proc. Natl. Acad. Sci. U. S. A. 111*, E888.
- (39) Meng, X., Zhou, J., Tang, J., Li, B., de Oliveira, M. V. V, Chai, J., He, P., and Shan, L. (2016) Ligand-Induced Receptor-like Kinase Complex Regulates Floral Organ Abscission in Arabidopsis. *Cell Rep.* 14 (14), 1330–1338.
- (40) Red Brewer, M., Choi, S. H., Alvarado, D., Moravcevic, K., Pozzi, A., Lemmon, M. A., and Carpenter, G. (2009) The juxtamembrane region of the EGF receptor functions as an activation domain. *Mol. Cell* 34, 641–651.
- (41) Dawson, J. P., Berger, M. B., Lin, C. C., Schlessinger, J., Lemmon, M. A., and Ferguson, K. M. (2005) Epidermal growth factor receptor dimerization and activation require ligand-induced conformational changes in the dimer interface. *Mol. Cell. Biol.* 25, 7734—7742.
- (42) Sun, W., Cao, Y., Jansen Labby, K., Bittel, P., Boller, T., and Bent, A. F. (2012) Probing the Arabidopsis flagellin receptor: FLS2-FLS2 association and the contributions of specific domains to signaling function. *Plant Cell* 24, 1096–1113.
- (43) Li, C., Yeh, F. L., Cheung, A. Y., Duan, Q., Kita, D., Liu, M. C., Maman, J., Luu, E. J., Wu, B. W., Gates, L., Jalal, M., Kwong, A., Carpenter, H., and Wu, H. M. (2015) Glycosylphosphatidylinositol-anchored proteins as chaperones and co-receptors for FERONIA receptor kinase signaling in Arabidopsis. *eLife* 4, 06587.
- (44) Du, C., Li, X., Chen, J., Chen, W., Li, B., Li, C., Wang, L., Li, J., Zhao, X., Lin, J., Liu, X., Luan, S., and Yu, F. (2016) Receptor kinase complex transmits RALF peptide signal to inhibit root growth in Arabidopsis. *Proc. Natl. Acad. Sci. U. S. A.* 113, E8326–E8334.